

© 2018 American Meteorological Society. For information regarding reuse of this content and general copyright information, consult the [AMS Copyright Policy](https://www.ametsoc.org/PUBSReuseLicenses) ([www.ametsoc.org/PUBSReuseLicenses](https://www.ametsoc.org/PUBSReuseLicenses)).

# Influence of Soil Properties in Different Management Systems: Estimating Soybean Water Changes in the Agro-IBIS Model

Virnei Silva Moreira,<sup>a</sup> Luiz Antonio Candido,<sup>b</sup>  
Debora Regina Roberti,<sup>c,f</sup> Geovane Webler,<sup>c</sup>  
Marcelo Bortoluzzi Diaz,<sup>c</sup> Luis Gustavo Gonçalves de Gonçalves,<sup>d</sup>  
Raphael Pousa,<sup>e</sup> and Gervásio Annes Degrazia<sup>c</sup>

<sup>a</sup> Universidade Federal do Pampa, Itaqui, Rio Grande do Sul, Brazil

<sup>b</sup> Instituto Nacional de Pesquisas da Amazônia, Manaus, Amazonas, Brazil

<sup>c</sup> Departamento de Física, Universidade Federal de Santa Maria, Santa Maria, Rio Grande do Sul, Brazil

<sup>d</sup> Centro de Previsão de Tempo e Clima (CPTEC/INPE), Cachoeira Paulista, São Paulo, Brazil

<sup>e</sup> Universidade Federal de Viçosa, Viçosa, Minas Gerais, Brazil

Received 19 December 2016; in final form 21 September 2017

**ABSTRACT:** The water balance in agricultural cropping systems is dependent on the physical and hydraulic characteristics of the soil and the type of farming, both of which are sensitive to the soil management. Most models that describe the interaction between the surface and the atmosphere do not efficiently represent the physical differences across different soil management areas. In this study, the authors analyzed the dynamics of the water exchange in

---

<sup>f</sup> Corresponding author: Debora Regina Roberti, [debora@ufsm.br](mailto:debora@ufsm.br)

the agricultural version of the Integrated Biosphere Simulator (IBIS) model (Agro-IBIS) in the presence of different physical soil properties because of the different long-term soil management systems. The experimental soil properties were obtained from two management systems, no tillage (NT) and conventional tillage (CT) in a long-term experiment in southern Brazil in the soybean growing season of 2009/10. To simulate NT management, this study modified the top soil layer in the model to represent the residual layer. Moreover, a mathematical adjustment to the computation of leaf area index (LAI) is suggested to obtain a better representation of the grain fill to the physiological maturity period. The water exchange dynamics simulated using Agro-IBIS were compared against experimental data collected from both tillage systems. The results show that the model well represented the water dynamics in the soil and the evapotranspiration (ET) in both management systems, in particular during the wet periods. Better results were found for the conventional tillage management system for the water balance. However, with the incorporation of a residual layer and soil properties in NT, the model improved the estimation of evapotranspiration by 6%. The ability of the Agro-IBIS model to estimate ET indicates its potential application in future climate scenarios.

**KEYWORDS:** In situ observations; Land surface model; Model evaluation/performance

## 1. Introduction

The assessment of land surface–atmosphere interactions and consequent climate impacts on agroecosystems through modeling studies do not generally take into account the contribution from soil management practices (Bagley et al. 2015). Recently, land surface models (LSMs) have been developed in order to simulate different crop types and their responses to climatic variability, resulting in improved early detection of agricultural drought with further mitigation responses (Kucharik et al. 2000; Kucharik and Brye 2003; Kucharik and Twine 2007; Lokupitiya et al. 2009; Cuadra et al. 2012; Mo et al. 2011; Ingwersen et al. 2011; Crow et al. 2012; Song et al. 2013; Twine et al. 2013). These models take into account crop phenological and physiological processes and their influence on surface water, energy, and carbon exchanges. The results indicate that the models are able to consistently simulate the processes related to the development of crops. However, the impact of different soil management is still not well known in these LSMs. Soil properties can contribute to a greater impact in the water budget compared to the impacts of vegetation properties (Liang and Guo 2003). Chen et al. (2015) demonstrated that there is a high sensitivity of the soil parameters to the soil moisture simulation.

Agriculture production depends on an adequate supply of water to the rooting zone (Gaofeng et al. 2014). Current efforts have been concentrated on maximizing the infiltration of the water in the soil and, consequently, minimizing the moisture loss through runoff and/or evaporation ( $E$ ). Different techniques to decrease the water use in agriculture and increase the productivity are constantly being developed and tested, including exploring the differences between conventional tillage (CT) and no tillage (NT) crop systems. The conventional cropping system, with intense soil disturbance characterized by the use of a plow, can create surface layers with lower density, less aggregation, and high permeability (Reichert et al. 2009). The nonrevolving soil in NT, without plowing, tilling, or removal of the

straw of the previous crop from the soil surface, acts as an energy dissipater, protects the soil from the impact caused by rain, and prevents surface sealing. It reduces the pore obstruction at the soil surface, favoring an increase in the water infiltration rate and consequently decreasing water erosion (Kay and VandenBygaart 2002). According to Costa et al. (2003) the adoption of NT promotes an improvement in soil structure and physical properties, mainly because of the influence of crop residues on the surface.

Changes in soil structure that are induced by NT and CT management can lead to significant differences in the aggregation, density, and discontinuity of pores that directly affect the components of the water balance of the system, such as runoff, soil water content, and evapotranspiration (ET; Blevins et al. 1990; De Vita et al. 2007; Almaraz et al. 2009; Verkler et al. 2008; Tormena et al. 2002). Weblar et al. (2017, manuscript submitted to *Adv. Meteor.*) showed that the presence of a straw layer can increase the soil volumetric water content (VWC) by 5%–15% and increase the surface albedo by 10%, thus leading to lower skin and soil temperatures. The evaporation of soil water depends on the management system, mainly when a fraction of ground surface is not covered by plants. Less water loss to evaporation occurs when the straw layer is present (Allen et al. 1998). The exposure of soil to meteorological forcing, such as wind and solar radiation, makes evaporation easier when tilling occurs (Allen et al. 1998). The transpiration ( $T$ ) process is affected more significantly by the availability of soil water than by the residual layer over the soil. However, the no tillage soil with the straw layer can modify the soil structure over time (Moreira et al. 2015).

The objective of this study was to assess the impacts of a detailed description of soil properties in the estimation of water changes by the agricultural version of the Integrated Biosphere Simulator (IBIS) model (Agro-IBIS) for two soybean cropping systems. To represent the residual layer in the models, we modified the top model soil layer. Additionally, a new leaf area index (LAI) formulation for soybean grain fill to the physiological maturity period is proposed. The model is then calibrated, and the simulation results are compared with the measured soil water content, evapotranspiration, drainage and runoff, and leaf area index data obtained from the two cropping systems. This evaluation was performed using experimental data from the soybean [*Glycine max* (L.) Merrill] growing season during 2009/10 in southern Brazil under two soil management systems: NT and CT. Evapotranspiration observations were obtained using the eddy covariance method. A discussion regarding the differences in the estimated evapotranspiration partition (evaporation and transpiration) for the soybean growing season between NT and CT management is also presented.

## 2. Materials and methods

### 2.1. Site and crop description

The study area is located at the Cooperativa Central Gaucha Ltda -Tecnologia/Fundacao Centro De Experimentação E Pesquisa (CCGL-TEC/FUNDACEP) in Cruz Alta (28°36'S, 53°40'W; 425 m), Rio Grande do Sul, the southernmost state in Brazil. The climate is Cfa (according to Köppen climate classification; Peel et al. 2007) subtropical humid. Experiments with crop rotation are conducted in each

pair of plots: one with an NT system the other with a CT system (Chavez et al. 2009; Bortolotto et al. 2015). A 3-yr rotation has occurred in the experimental area since 1985. We evaluated the pair of plots with the following sequence: year 1 consists of common vetch (*Vicia sativa* L.) mixed with black oats (*Avena strigosa* L.) in winter and maize (*Zea mays* L.) in summer; year 2 consists of wheat in winter and soybean in summer; and year 3 consists of black oats in winter and soybean in summer. The soybean in the last period (year 3) was analyzed here (soybean growing season 2009/10).

The soybean cultivar used in the experiment was FUNDACEP 53RR, with early maturity. The plant cycle in the experimental site started on 14 December 2009 (sowing). On 13 April 2010, physiological maturity was identified, and the harvest was held on 28 April 2010. The soybean growth stages were determined using the phenological scale proposed by Fehr and Caviness (1977). Details about the site and these growing season characteristics are given in Moreira et al. (2015).

Before the soybean growing season of 2009/10, both plots (CT and NT) were cultivated with black oats, which were sowed on 28 July 2009 and desiccated on 10 November 2009. Desiccation means the application of an herbicide to dry the crop. This crop is used only as crop residue. In the CT, the soil was tilled with a plow on 8 December 2009. Generally, in this region, soybean is sown some days after black oat desiccation (beginning in November), but because of excessive rainfall during November 2009 (381.6 mm), the soybean sowing was delayed.

## 2.2. Experimental data

### 2.2.1. Meteorological measurements

Two eddy covariance (EC) towers were installed in the experimental area: one in the NT and the other in the CT systems. Measurements were taken from 19 December 2009 to 28 April 2010. Sensors for each EC tower included a 3D sonic anemometer (Campbell Scientific, Inc., CSAT 3) for measurements of the wind turbulence components and an infrared open-path gas analyzer (Li-Cor, Inc., LI7500) to measure the H<sub>2</sub>O concentrations, both of which were placed at a height of 2.5 m and sampled at a 10-Hz frequency. The latent heat flux (LE) was estimated by the eddy covariance method (Baldocchi et al. 1988) using Li-Cor EddyPro software, version 5.1.1., to compute the fluxes over a 30-min interval. The fluxes were corrected for inadequate sensor frequency response following standard methods in addition to despiking, coordinate rotation, and air density corrections (Webb et al. 1980; Baldocchi et al. 1988; Wyngaard 1990; Aubinet et al. 1999). Periods with physically inconsistent values (i.e.,  $LE < -50 \text{ W m}^{-2}$  or  $LE > 1000 \text{ W m}^{-2}$ ) were discarded. The footprint filter was used when the data came from outside the soybean border for NT and CT (Hsieh et al. 2000). This quality control procedure left a total time gap in the data of approximately 66% with respect to the entire period. The gap filling applied to the LE fluxes was provided by the REddyProc package available in the RStudio software based on procedures described by Reichstein et al. (2005).

A meteorological station with continuous measurements starting in 1974 is located approximately 400 m from the eddy covariance towers. The weather station provides the atmospheric data to force the Agro-IBIS model (air temperature, wind speed, precipitation, global radiation, relative humidity, and atmospheric pressure).

**Table 1. Soil hydrophysical characteristics for experimental NT and CT plot sites. Sand fraction (%), silt fraction (%), clay fraction (%), soil water content at saturation  $\theta_s$  ( $\text{cm}^3 \text{cm}^{-3}$ ), saturated hydraulic conductivity  $K_s$  ( $\text{m s}^{-1}$ ), air entry water potential  $\psi_s$  (m- $\text{H}_2\text{O}$  Campbell's exponent  $b$ ).**

	Sand	Silt	Clay	$\theta_s$	$K_s$	$\psi_s$	$b$
CT	0.24	0.29	0.45	0.615	$3.67 \times 10^{-05}$	0.11	8.125
NT	0.26	0.31	0.43	0.545	$2.75 \times 10^{-06}$	0.11	7.875

More details about the experimental design can be found in [Webler et al. \(2012\)](#) and [Moreira et al. \(2015\)](#).

### 2.2.2. Measurement of LAI

The soybean LAI was obtained by collecting four plants distributed randomly in each plot. The leaves from each plant were removed, stretched over a known area, and photographed. The pictures were then processed through the software Assess 2.0 (an image analysis software for plant disease quantification; [Lamari 2008](#)), which determined the surface area covered by leaves, therefore allowing calculation of the LAI.

### 2.2.3. Soil hydrology

The soil type in the plot sites is clay (rhodic ferralsol—FAO soil taxonomy—or Typic Haplorthox—U.S. soil taxonomy), deep and without slope, differing only in the hydrophysical characteristics associated with the soil management in NT and CT. The physical properties of the soil were obtained in the laboratory from field samples collected from layers from 0- to 0.20-m depth and from 0.20- to 0.50-m depth for both management systems. In this work, the soil properties are averaged over the entire depth. The properties include texture (sand, silt, and clay fractions), soil water content at saturation  $\theta_s$ , and saturated hydraulic conductivity  $K_s$  (see [Table 1](#)). The  $K_s$  was determined using a falling head permeability meter ([Gubiani et al. 2010](#)).

The soil water content was determined experimentally on a scale from 0 to  $1 \text{ m}^3 \text{ m}^{-3}$  through the time domain reflectometry (TDR) sensors (Campbell Scientific model CS616-L) installed with a slope of  $45^\circ$  to cover the 0–0.20-m depth and in the vertical position to cover the 0.20–0.50-m depth near the micrometeorological towers in both plots. The measurements were initiated on 19 December 2009, at the emergence of soybean, and continued until 25 April 2010, 3 days before harvest. Soil drainage was calculated by measuring the water excess between 0.2 and 0.5 m (Darcy's law). Runoff measurements were completed using eight galvanized steel structures installed in the experimental area (four in each planting system). After each rainy day, the containers were collected, and water losses were computed. More details of soil hydrology are reported in [Moreira et al. \(2015\)](#).

## 2.3. Agro-IBIS model

The Agro-IBIS model ([Kucharik and Brye 2003](#)) is a version of the IBIS model ([Foley et al. 1996](#)) that includes the representation of agricultural crops. It includes 12 natural and 6 crop plant functional types ([Kucharik and Brye 2003](#); [Vanloocke](#)

et al. 2010; Cuadra et al. 2012). Soybean (*Glycine max*), maize (*Zea mays*), wheat (*Triticum vulgare* Vill), *Miscanthus x. giganteus*, and switchgrass and sugarcane (*Saccharum officinarum* L.) representations are also included. The Agro-IBIS model uses the same set of equations to represent the physical and biophysical processes that simulate energy and mass balances of natural and agricultural ecosystems. The equations are described in detail in Foley et al. (1996), Kucharik et al. (2000), and Kucharik and Brye (2003). The model represents land surface processes related to energy, water, carbon, and momentum exchanges between the soil, vegetation (canopy and root system), and the atmosphere. The model also simulates the canopy physiology (photosynthesis and stomatal conductance), phenology, vegetation dynamics (carbon allocation, competition between plants), and carbon balance (net primary production, carbon allocation, soil carbon, and organic matter decomposition), operating from hourly to yearly time scales. This approach permits the coupling of the ecological, biophysical, and physiological phenomena that occur at different time scales. The model output can provide daily values for crop productivity, dry matter production (leaves, stems, roots and grains), LAI, evapotranspiration, and carbon flux. The soil is represented by 11 layers totaling 2.5 m in depth. The Agro-IBIS model was calibrated and validated for soybean for conditions in North and South America (Kucharik and Twine 2007; Twine et al. 2013; Webler et al. 2012).

### 2.3.1. Residual layer in the model

No physical processes linked to different soil management systems are characterized in original version of Agro-IBIS. In this work, we follow Kucharik et al. (2013) to represent a residual layer over the soil. The parameters describing the soil surface layer, from 0 to 0.05 m, were modified to represent the physical effects of the residual layer (straw layer). The values of thermal conductivity, specific heat, porosity, and albedo were modified to represent the bare soil (CT system) and the straw (NT system).

### 2.3.2. Soil parameters adjustment

The functions used by Agro-IBIS to describe the relationship between the volumetric soil water content  $\theta$  ( $\text{m}^3 \text{m}^{-3}$ ) and its soil matric potential  $\psi$  (kPa), that is, the soil water retention curve, are given by equations from Campbell (1974), defined by

$$\theta = \theta_s \quad \text{if} \quad \psi \geq \psi_s \quad \text{and} \quad (1)$$

$$\theta = \theta_s \left( \frac{\psi}{\psi_s} \right)^{-1/b} \quad \text{if} \quad \psi < \psi_s, \quad (2)$$

where  $\theta_s$  is the soil water content at saturation,  $\psi_s$  is the air entry water potential, and  $b$  is the empirical Campbell constant. The parameter  $b$  represents the slope of the water retention curve adjusted to experimental data and, in this work, was obtained by considering data from 0- to 0.50-m depth for the water soil content  $\theta$  and the linear fit of the retention curve.

### 2.3.3. Evapotranspiration

The Agro-IBIS model considers only a canopy level for the crop simulation. Turbulent flux and the wind through the canopy are simulated using a logarithmic profile. The turbulent fluxes between the soil and the canopy are represented as a function of wind speed. Hydrological processes are simulated by considering the interception of precipitation and retention in the canopy, formation of surface reservoirs, infiltration, the water flux between soil layers, percolation, evaporation of intercepted water, evaporation of water at the soil surface, and transpiration of the plant (Foley et al. 1996).

The soil water evaporation is calculated by using the near-land surface air relativity ( $\alpha$  method), calculated as a function of the moisture availability parameter ( $\beta$  method; Mahfouf and Noilhan 1991). In addition, Agro-IBIS estimates the evaporation on wet surfaces and plant transpiration by leaf area unit in the upper and lower canopies (Pollard 1995). The transpiration is calculated using the atmospheric demand by means of a vapor gradient between the atmosphere and the stomatal cavity and the energy available (Abramopoulos et al. 1988).

### 2.3.4. LAI adjustment

The Agro-IBIS model divided the growing season in three different phases to estimate the LAI: phase 1 is from planting to leaf emergence; phase 2 is from leaf emergence to the beginning of grain fill (LAI accumulation), when LAI is calculated as the product of the specific leaf area and the accumulated leaf carbon; and phase 3 is the grain fill to physiological maturity and subsequent harvest (LAI decline). Previous studies, such as Kucharik and Twine (2007) and Webler et al. (2012), described an overestimation of LAI simulation in phase 3. The original equation for LAI in the Agro-IBIS model for phase 3 is

$$LAI = LAI \left[ 1 - \left( \frac{gdd_{plant} - hui_{grain}}{0.55gdd_{maturity}} \right)^x \right], \quad (3)$$

where  $gdd_{plant}$  is the daily growing degree-days (GDD) at the senescence stage,  $hui_{grain}$  is the GDD at the beginning of the grain fill stage,  $gdd_{maturity}$  is the GDD until maturity, and  $x$  is the coefficient of adjustment and is not dependent on the cultivar. We propose here a new equation with a dynamic exponent that reduces the LAI from grain fill until the end of the growing season (phase 3 only):

$$LAI_j = LAI_{j-1} \left( 1 - \frac{gdd_{plant} - hui_{grain}}{0.55gdd_{maturity}} \right)^{\{a[(gdd_{plant} - hui_{grain})/(gdd_{maturity})]\}}, \quad (4)$$

where  $a$  is a constant. In Equation (4), the ratio between the difference of  $gdd_{plant}$  and  $hui_{grain}$  with  $gdd_{maturity}$  becomes positive, while subtraction of the unit decreases after physiological maturity. This relationship allowed the establishment of a dynamic exponent that is smaller than the unit value that decreases until the end of the crop cycle. The new exponent determines the rate at which the LAI, after the

**Table 2. Top soil layer modification in the Agro-IBIS model to represent the NT and CT management systems.**

Quantity	NT		CT	
	Value	Reference	Value	Reference
Thermal conductivity (W m <sup>-2</sup> K <sup>-2</sup> )	0.126	Chung and Horton (1987)	0.267	Agro-IBIS (default)
Specific heat (J kg <sup>-2</sup> K <sup>-2</sup> )	1200	Van Wijk and De Vries (1963)	900	Agro-IBIS (default)
Porosity	0.95	Moreira et al. (2015)	0.48	Moreira et al. (2015)
Albedo	0.16	Webler et al. (2017, manuscript submitted to <i>Adv. Meteor.</i> )	0.13	Webler et al. (2017, manuscript submitted to <i>Adv. Meteor.</i> )

beginning grain fill, occurs. This parameter  $a$  is dependent on the cultivar and needs to be obtained by calibration.

## 2.4. Simulations

Two numerical simulations were performed using the same atmospheric forcing:

- 1) CT simulation used the soil hydrophysical characteristic for CT (see Table 1) and bare soil values for the top soil surface (see Table 2), and
- 2) NT simulation used soil hydrophysical characteristic for NT (see Table 1), and the top soil surface was modified to represent the straw layer (see Table 2).

For both simulations, the new representation of LAI after beginning grain fill was used [Equation (4)]. The base temperature was set to 10°C, while the forcing temperature was used to calculate the GDD. The total GDD for the soybean growing season during 2009/10 was 1681:  $gdd_{maturity}$ . After the accumulation of 1206.8 GDD, the grain fill stage huigrain began. The  $a$  coefficient was adjusted by the least squares error between simulated and experimental LAI for CT and NT, obtaining values of  $a = 9.5$  and  $a = 10.9$ , respectively.

The Hanna (1989) metrics used to evaluate the simulations with experimental values are the root mean square (quadratic mean) error (RMSE), normalized mean square (quadratic mean) error (NMSE), correlation coefficient ( $R$ ), and fractional bias (FB).

## 3. Results and discussions

### 3.1. Weather conditions

Figure 1 shows the precipitation and temperature for the 2009/10 soybean growing season at the site of Cruz Alta and monthly climate conditions. The soybean growing season was characterized by more intense rainfall until 40 days

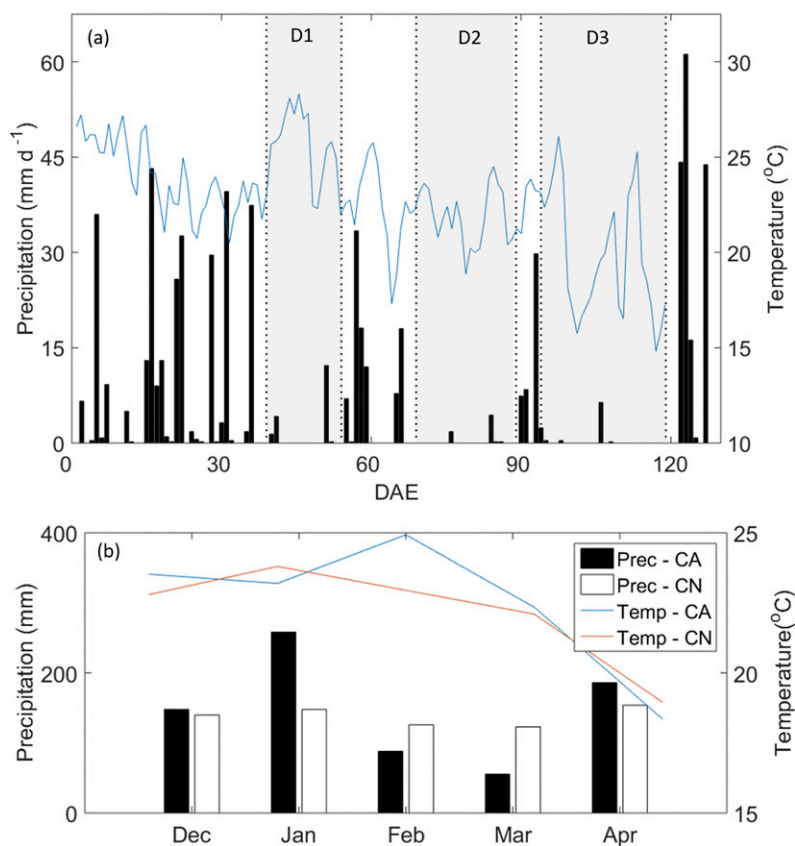


**Figure 1. (a) Seasonal distributions of temperature and precipitation for the 2009/10 soybean growing season in southern Brazil. (b) Monthly mean temperature and accumulated monthly precipitation for Cruz Alta (CA) and climatic normal (CN).**

after emergence (DAE; until 28 January), with a total of 310 mm, which represented 63% of the precipitation of the entire cycle (492 mm integrated in the soybean growing season). In January, the precipitation was 75% higher than the long-term average; however, in February and March, the precipitation was 30% and 55% less than long-term averages, respectively. The mean temperature was 22.5°C in the period. In February, the temperature was 2°C higher than the long-term average. In the other months, the temperature was similar to the climatic mean. More detailed environmental conditions during the period of this study are described in [Moreira et al. \(2015\)](#).

To better analyze the results of the soil water content, the period was separated into wet and dry periods as follows: The four wet periods were W1 = 0 (19 December) to 40 (28 January) DAE, W2 = 55 (11 February) to 70 (26 February) DAE, W3 = 90 (18 March) to 95 (23 March) DAE, and W4 = 120 (20 April) to 129 DAE (28 April). The three dry periods (periods with more than 10 days without rainfall) were D1 = 40 (28 January) to 55 (11 February) DAE, D2 = 70 (26 February) to 90 DAE (18 March), and D3 = 95 (23 March) to 120 (20 April) DAE.

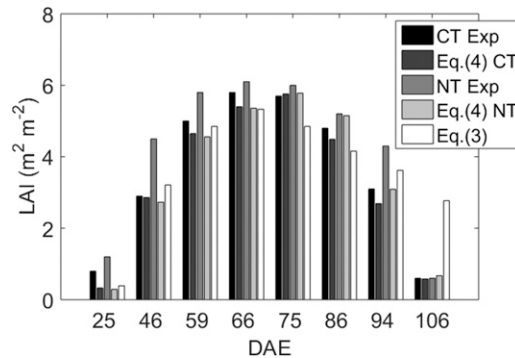


**Figure 2.** Simulated and experimental LAI for NT and CT for the 2009/10 soybean growing season in southern Brazil using Equation (4). The LAI simulated using Equation (3) is also presented.

### 3.2. LAI

The difficulty of the Agro-IBIS to simulate the LAI decrease after the grain fill period has been noted by a number of previous studies (Kucharik and Twine 2007; El Maayar and Sonnentag 2009; Webler et al. 2012). A comparison between the simulated and experimental LAI is shown in Figure 2. We also show the difference of the LAI estimated using Equations (3) and (4) to represent the period of after the beginning of grain fill (after 88 DAE). The period before used the original LAI equations. Equation (3) was used for the CT simulation, as described in section 2.4. The LAI obtained with Equation (3) does not follow the behavior of the experimental LAI, exceeding the LAI values by approximately  $2 \text{ m}^2 \text{ m}^{-2}$  at the end of growing season.

Comparing the LAI simulation using Equation (3) with the experimental LAI for CT and NT, the RMSE was  $0.76$  and  $0.86 \text{ m}^2 \text{ m}^{-2}$ , respectively. Using Equation (4), the RMSE between the simulated and experimental LAI was determined to be  $0.69 \text{ m}^2 \text{ m}^{-2}$  for NT and  $0.23 \text{ m}^2 \text{ m}^{-2}$  for CT.

The LAI experimental values for the NT system are greater than those for CT for all observation dates. The model [using Equation (4)] was able to reproduce this pattern. On the last measurement date (106 DAE), the simulated LAI are very similar to experimental values. Simulated LAI also shows a high correlation with the observations (0.99 for CT and 0.95 for NT); although, it generally underestimates the observations by 8% in the CT plot and by 15% in the NT plot. Therefore, even accounting for differences between the simulations, both simulations better represent the LAI CT experimental values.

### 3.3. Soil water content dynamics

The soil experimental characteristics found in CT and NT are similar in sand, silt, and clay and air entry water potential (Table 1). The larger differences between NT and CT are found in the parameters for soil water content at saturation  $\theta_s$ ,

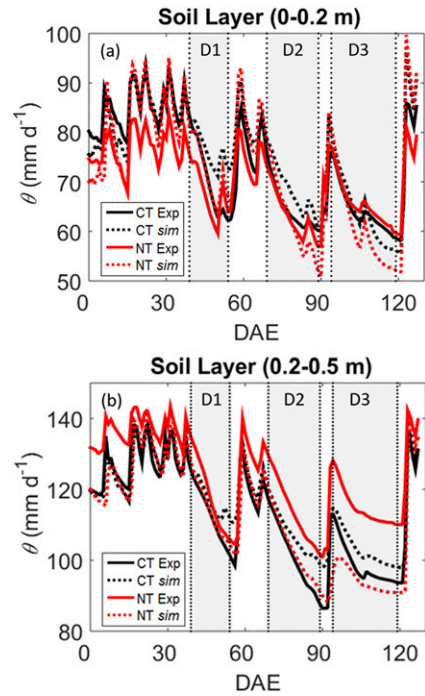


**Figure 3. Simulated and experimental soil water content  $\theta$  daily average for (a) 0–0.2-m soil layer and (b) 0.2–0.5-m soil layer.**

saturated hydraulic conductivity  $K_s$ , and empirical Campbell constant  $b$ . These parameters are greater in CT than in NT (Table 1).

The observed and simulated soil water content for both CT and NT systems at layers from 0- to 0.2-m depth and from 0.2- to 0.5-m depth are shown in Figures 3a and 3b. In CT, the model performs better for soil water content simulations during wet periods compared to dry periods for both layers. The statistical indices are also very similar (Table 3) for soil layers during both wet and dry periods. In dry periods, the model overestimates the experimental data more than in wet periods, which can be confirmed by the greater negative FB in dry periods (Table 3). In the D3 period for the first soil layer (0–0.20 m) in CT, the simulated soil water content

**Table 3. Statistical analysis of the soil water content using RMSE, NMSE,  $R$ , and FB for the 2009/10 soybean growing season in southern Brazil for 0–0.20- and 0.20–0.50-m soil layers in CT and NT management systems.**

		Wet periods				Dry periods			
		RMSE	NMSE	$R$	FB	RMSE	NMSE	$R$	FB
0–0.2 (m)	CT	4.37	0.05	0.89	–0.02	4.66	0.07	0.86	–0.04
	NT	7.66	0.10	0.91	–0.006	4.93	0.08	0.88	0.03
0.2–0.5 (m)	CT	4.67	0.04	0.95	–0.01	4.66	0.07	0.86	–0.04
	NT	12.31	0.10	0.88	0.004	4.93	0.08	0.87	0.03

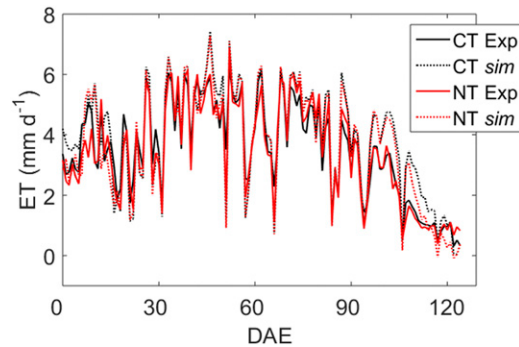


Figure 4. Daily average of experimental and simulated evapotranspiration.

undergoes a greater reduction compared to the experimental data, which was certainly influenced by a long period without precipitation (almost 30 days).

The simulated soil water content for NT overestimates the experimental values only during the wet periods for the first soil layer (0–0.20 m;  $FB < 0$ , in Table 3). For other situations, the model underestimates the experimental soil water content. The errors (RMSE and NMSE) are larger in the second soil layer (0.2–0.5 m).

During the wet periods, for both soil layers, the model results (for NT and CT) present similar behavior. However, during dry periods, the magnitude of the results is different. For all simulations, the correlation coefficient  $R$  is greater than 0.85. The pattern of the experimental data is well represented by the model, whereas in the second layer, the experimental NT presents larger values of soil water content than CT, and the simulated results present the CT with more water in this layer. This result can be explained by the experimental values of saturated hydraulic conductivity  $K_s$  (Table 1). High values of  $K_s$  mean the soil has a greater capacity to conduct water, either to the surface (dry periods) or to deep drainage (wet period; Bhattacharyya et al. 2006).

### 3.4. Evapotranspiration

The water requirement for the soybean growing season varies with the different stages of development and is determined by water losses through evapotranspiration, plant water conditions, and the soil management system. Evapotranspiration consists of the evaporation of water intercepted by leaves, soil water evaporation, and transpiration. In this study, we used the eddy covariance method to estimate the evapotranspiration. This technique integrates all components of evapotranspiration (soil evaporation, leaf interception, and transpiration). In a condition without soil water stress, the variability of evapotranspiration is associated with rainfall and crop development stages. A detailed description of hydrophysical characteristics of the soil in Agro-IBIS when simulating the soybean growing season did not present significant differences between ET for both planting systems (Figure 4). After 100 DAE, the NT simulation represents the decay in ET through the days similarly to the experimental data.

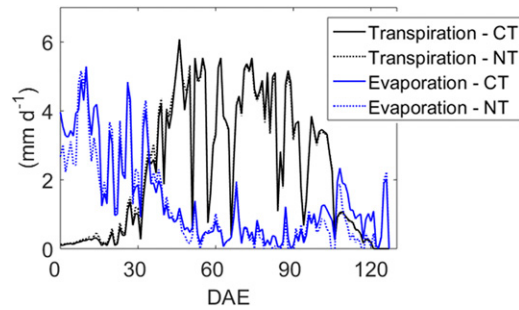


Figure 5. Simulated daily averages of evaporation and transpiration for CT and NT.

Agro-IBIS overestimates the ET in the two simulations (4.0% for NT and 7.7% CT). In general, the NT simulations for ET present a better correlation coefficient  $R$  with the experimental data (NT:  $R = 0.84$ ; CT:  $R = 0.80$ ). The integrated ET in the 2009/10 soybean growing season for CT and NT management systems presents 3% differences between experimental results and simulations. However, the magnitude of the difference between experimental and simulated ET was 6% for both management systems.

In general, no physical process linked to different soil management systems is characterized in land surface models. With the results presented here, a 10% error in the ET estimation is found using CT simulations to represent an NT experiment, which represents a difference of 44.85 mm of ET in the 2009/10 soybean growing season. However, the improvement in the estimate of ET using the NT simulation was approximately 6%.

### 3.5. Evaporation and transpiration

The Agro-IBIS representation for evaporation and transpiration for NT and CT simulations is represented in Figure 5. The direct evaporation and transpiration were not measured experimentally. The integrated values of  $E$  and  $T$  and its ET ratio are presented in Table 4. The greater differences between the results are in the evaporation values (12% greater in CT). This difference is evident at the beginning and end of the growing season, periods with small LAI (Figure 5), and when the

Table 4. ET,  $E$ , and  $T$  for the 2009/10 soybean growing season in CT and NT management systems using results of the simulation and experimental data (in parentheses). Period from 19 Dec 2009 to 25 Apr 2010.

	CT		NT	
	Accumulated	Daily mean	Accumulated	Daily mean
ET (mm)	474.25 (423.31)	3.70 (3.31)	448.46 (410.88)	3.50 (3.21)
$E$ (mm)	179.55	1.40	157.17	1.23
$T$ (mm)	294.67	2.30	291.22	2.27
$E/ET$	37.8%		35.0%	
$T/ET$	62.1%		65.0%	

**Table 5. Components of the water balance for the 2009/10 soybean growing season under NT and CT, in units of mm, for experimental and simulated results. Period from 19 Dec 2009 to 25 Apr 2010 (*P* is precipitation, *ET* is evapotranspiration, *Rs* is surface runoff, *D* is drainage in the profile, and *WB* is water balance).**

		Input <i>P</i>	Output			WB <i>P-ET-Rs-D</i>
			<i>ET</i>	<i>Rs</i>	<i>D</i>	
NT	Experimental	654.8	429.4	12.1	108.9	104.4
	Simulated	654.8	448.46	19.88	210.22	-23.76
CT	Experimental	654.8	440.3	20.6	168.4	25.5
	Simulated	654.8	474.25	19.56	183.18	-22.19

crop residues on the top of the soil layer can directly influence surface water process, decreasing the *E* in NT. The overestimation of *ET* in periods with small LAI values (the beginning and the end of growing season) in [Figure 4](#) can also represent an overestimation of *E* in the model.

The partitioning of *ET* into *E* and *T* are similar of other works on soybean. [Wei et al. \(2015\)](#) found the relationship *E/ET* to be between 0.38 and 0.28 for CT, in agreement with our results ([Table 4](#)). The *E/ET* partition is slightly smaller in the NT simulation. This behavior is expected since the model represents the crop residues on the soil surface. These residues can influence the radiation and energy balance, and the aerodynamic and hydraulic resistance, decreasing evaporation from the soil even more if it were implemented ([Bhattacharyya et al. 2006](#); [Kozak et al. 2007](#); [van Donk et al. 2010](#); [Schwartz et al. 2010](#)).

### 3.6. Water balance

The water balance analyses were performed from 19 December 2009 to 25 April 2010, the period when all the variables were measured. The experimental and simulated results are presented in [Table 5](#). While the experimental data presented a positive water balance, in both systems, the model presented a negative water balance, with similar values. The greatest difference between the experimental and simulated values was found in the drainage for NT; in CT, the difference in drainage is approximately 9%, while in NT, the difference is approximately 93%. In [Figure 3](#), we can see the faster soil drying in dry periods for NT, which is directly related to high drainage, since the *ET* differences are smaller.

The lower runoff in the NT experiment relative to the CT experiment ([Table 5](#)) reflects the effect of the residual straw layer on the higher water retention, favoring higher infiltration [also described by [Olivier and Singels \(2012\)](#)]. The runoff was very similar between the two simulations where CT was slightly closer to the experimental data. On the other hand, the runoff for simulated NT presented a 65% difference relative to the observed data. These differences between runoff simulated and observed can be attributed to the lack of parameterization of high water retention in the model, which only considers runoff after soil saturation ([Kucharik and Brye 2003](#)). In the model formulation, the loss of water by drainage to the deeper layers is primarily determined by the soil hydraulic conductivity. Consequently, the differences in simulated drainage and runoff caused by the higher

hydraulic conductivity of the soil in NT (Table 1) favored the greater losses to the deeper soil layers. The inclusion of the residual straw layer did not affect soil infiltration.

The results presented here agree with Chen et al. (2015) using the IBIS model. They concluded that the land surface schemes may be ineffective for predicting the hydrology unless the soil moisture is accurately estimated. Therefore, the crop residues layer implemented in the model did not present the expected reduction in water lost to runoff. This result may be because the modification occurred principally in thermal properties, although the porosity value was doubled.

Infiltration and redistribution of water in the soil depend critically on its material and hydraulic properties. Furthermore, most soils generally are classified according to the content of clay, sand, and silt, following a texture scheme developed by the USDA (Dingman 2002); although, the amount of organic matter should be taken into account to properly determine the soil water matric suction. Many studies considered the presence of organic matter in the soil as a contaminant to the soil components (silt, clay, and sand) that generally increase the water holding capacity in the soil (Hudson 1994; Li et al. 2013). Other studies show that the water dynamics of residual/litter layer receive little attention or in many cases are completely disregarded, in several cases because of the lack of accurate field measurements (Gerrits et al. 2007; Lundberg et al. 1997).

## 4. Conclusions

In this work, the influence of a detailed description of soil properties in the estimation of soybean water was evaluated using the Agro-IBIS model. We used data for soybeans in southern Brazil under different soil management systems: no tillage and conventional tillage. A new description of LAI after the beginning of the grain fill period presents satisfactory results and correctly describes the decrease in LAI in this stage. Evapotranspiration is also consistent with results for both simulations. The use of the detailed description of soil properties and the residual layer for the NT simulations represents an improvement of 6% in the integrated ET over the growing season. However, significant differences in model simulations are present in the soil water content for dry and wet periods. The wet periods are well represented in CT simulations, while the model underestimates the NT simulations. In general, in dry periods, the model overestimates the soil water content for CT and underestimates it for NT management. Despite this bias, the model captured the seasonal fluctuations of soil drying and wetting for NT and CT simulations. The faster soil drying in the NT simulation represented the greater error in drainage.

The slope of the water retention curve was obtained by linearly fitting the retention curve using the water content information collected from 0- to 0.50-m depth. Nevertheless, further work should be devoted to the effect of the residual layer mass and type, combined with the rainfall intensity, on the maximum water storage capacity of the residual layer and its interception storage capacity.

Furthermore, the results presented here indicate that a more in-depth assessment of the source of errors needs to be further addressed for future model development. The current work focused on identifying such errors using RMSE statistics;

however, much can be achieved when random and systematic sources of errors are treated separately to properly tune the most relevant parameters as well as reduce structural model deficiencies within the presented soil management framework.

**Acknowledgments.** The authors acknowledge the Brazilian agencies CNPq (SWP 300442/2010-6), CAPES, and FAPERGS (1013380) for their financial support.

## References

- Abramopoulos, F., C. Rosenzweig, and B. Choudhury, 1988: Improved ground hydrology calculations for global climate models (GCMs): Soil water movement and evapotranspiration. *J. Climate*, **1**, 921–941, [https://doi.org/10.1175/1520-0442\(1988\)001<0921:IGHCFG>2.0.CO;2](https://doi.org/10.1175/1520-0442(1988)001<0921:IGHCFG>2.0.CO;2).
- Allen, R. G., L. S. Pereira, D. Raes, and M. Smith, 1998: Crop evapotranspiration: Guidelines for computing crop water requirements. FAO Irrigation and Drainage Paper 56, <http://www.fao.org/docrep/X0490E/X0490E00.htm>.
- Almaraz, J. J., X. Zhou, F. Mabood, C. Madramootoo, P. Rochette, B.-L. Ma, and D. L. Smith, 2009: Greenhouse gas fluxes associated with soybean production under two tillage systems in southwestern Quebec. *Soil Tillage Res.*, **104**, 134–139, <https://doi.org/10.1016/j.still.2009.02.003>.
- Aubinet, M., and Coauthors, 1999: Estimates of the annual net carbon and water exchange of forests: The EUROFLUX methodology. *Adv. Ecol. Res.*, **30**, 113–175, [https://doi.org/10.1016/S0065-2504\(08\)60018-5](https://doi.org/10.1016/S0065-2504(08)60018-5).
- Bagley, J. E., J. Miller, and C. J. Bernacchi, 2015: Biophysical impacts of climate-smart agriculture in the Midwest United States. *Plant Cell Environ.*, **38**, 1913–1930, <https://doi.org/10.1111/pce.12485>.
- Baldocchi, D. D., B. B. Hincks, and T. P. Meyers, 1988: Measuring biosphere-atmosphere exchanges of biologically related gases with micrometeorological methods. *Ecology*, **69**, 1331–1340, <https://doi.org/10.2307/1941631>.
- Bhattacharyya, R., V. Prakash, S. Kundu, and H. S. Gupta, 2006: Effect of tillage and crop rotations on pore size distribution and soil hydraulic conductivity in sandy clay loam soil of the Indian Himalayas. *Soil Tillage Res.*, **86**, 129–140, <https://doi.org/10.1016/j.still.2005.02.018>.
- Blevins, R. L., W. W. Frye, P. L. Baldwin, and S. D. Robertson, 1990: Tillage effects on sediment and soluble nutrient losses from a Maury silt loam soil. *J. Environ. Qual.*, **19**, 683–686, <https://doi.org/10.2134/jeq1990.00472425001900040009x>.
- Bortolotto, R. P., and Coauthors, 2015: Soil carbon dioxide flux in a no-tillage winter system. *Afr. J. Agric. Res.*, **10**, 450–457, <https://doi.org/10.5897/AJAR2014.9399>.
- Campbell, G. S., 1974: A simple method for determining unsaturated conductivity from moisture retention data. *Soil Sci.*, **117**, 311–314, <https://doi.org/10.1097/00010694-197406000-00001>.
- Chavez, L. F., T. J. C. Amado, C. Bayer, N. J. La Scala, L. F. Escobar, J. E. Fiorin, and B.-H. C. de Campos, 2009: Carbon dioxide efflux in a rhodic hapludox as affected by tillage systems in southern Brazil. *Rev. Bras. Cienc. Solo*, **33**, 325–334, <https://doi.org/10.1590/S0100-06832009000200010>.
- Chen, M., G. R. Willgoose, and P. M. Saco, 2015: Evaluation of the hydrology of the IBIS land surface model in a semi-arid catchment. *Hydrol. Processes*, **29**, 653–670, <https://doi.org/10.1002/hyp.10156>.
- Chung, S.-O., and R. Horton, 1987: Soil heat and water flow with a partial surface mulch. *Water Resour. Res.*, **23**, 2175–2186, <https://doi.org/10.1029/WR023i012p02175>.

- Costa, F. S., J. A. Albuquerque, C. Bayer, S. M. V. Fontoura, and C. Wobeto, 2003: Physical properties of a south Brazilian Oxisol as affected by no-tillage and conventional tillage systems. *Rev. Bras. Cienc. Solo*, **27**, 527–535, <https://doi.org/10.1590/S0100-06832003000300014>.
- Crow, W. T., S. V. Kumar, and J. D. Bolten, 2012: On the utility of land surface models for agricultural drought monitoring. *Hydrol. Earth Syst. Sci.*, **16**, 3451–3460, <https://doi.org/10.5194/hess-16-3451-2012>.
- Cuadra, S. V., and Coauthors, 2012: A biophysical model of sugarcane growth. *Global Change Biol. Bioenergy*, **4**, 36–48, <https://doi.org/10.1111/j.1757-1707.2011.01105.x>.
- De Vita, P., E. Di Paolo, G. Fecondo, N. Di Fonzo, and M. Pisante, 2007: No-tillage and conventional tillage effects on durum wheat yield, grain quality and soil moisture content in southern Italy. *Soil Tillage Res.*, **92**, 69–78, <https://doi.org/10.1016/j.still.2006.01.012>.
- Dingman, S. L., 2002: *Physical Hydrology*. 2nd ed. Prentice Hall, 646 pp.
- El Maayar, M., and O. Sonnentag, 2009: Crop model validation and sensitivity to climate change scenarios. *Climate Res.*, **39**, 47–59, <https://doi.org/10.3354/cr00791>.
- Fehr, W. R., and C. E. Caviness, 1977: Stages of soybean development. Cooperative Extension Service, Agriculture and Home Economics Experiment Station, Iowa State University Special Report 80, 11 pp.
- Foley, J. A., I. C. Prentice, N. Ramankutty, S. Levis, D. Pollard, S. Sitch, and A. Haxeltine, 1996: An integrated biosphere model of land surface processes, terrestrial carbon balance, and vegetation dynamics. *Global Biogeochem. Cycles*, **10**, 603–628, <https://doi.org/10.1029/96GB02692>.
- Gaofeng, Z., and Coauthors, 2014: Energy flux partitioning and evapotranspiration in a sub-alpine spruce forest ecosystem. *Hydrol. Processes*, **28**, 5093–5104, <https://doi.org/10.1002/hyp.9995>.
- Gerrits, A. M. J., H. H. G. Savenije, L. Hoffmann, and L. Pfister, 2007: New technique to measure forest floor interception—An application in a beech forest in Luxembourg. *Hydrol. Earth Syst. Sci.*, **11**, 695–701, <https://doi.org/10.5194/hess-11-695-2007>.
- Gubiani, P. I., D. J. Reinert, J. M. Reichert, N. S. Gelain, and J. P. G. Minella, 2010: Falling head permeameter and software to determine the hydraulic conductivity of saturated soil. *Rev. Bras. Cienc. Solo*, **34**, 993–997, <https://doi.org/10.1590/S0100-06832010000300041>.
- Hanna, S. R., 1989: Confidence limits for air quality model evaluations, as estimated by bootstrap and jackknife resampling methods. *Atmos. Environ.*, **23**, 1385–1398, [https://doi.org/10.1016/0004-6981\(89\)90161-3](https://doi.org/10.1016/0004-6981(89)90161-3).
- Hsieh, C.-I., G. Katul, and T. Chi, 2000: An approximate analytical model for footprint estimation of scalar fluxes in thermally stratified atmospheric flows. *Adv. Water Resour.*, **23**, 765–772, [https://doi.org/10.1016/S0309-1708\(99\)00042-1](https://doi.org/10.1016/S0309-1708(99)00042-1).
- Hudson, B. D., 1994: Soil organic matter and available water capacity. *J. Soil Water Conserv.*, **49**, 189–194.
- Ingwersen, J., and Coauthors, 2011: Comparison of Noah simulations with eddy covariance and soil water measurements at a winter wheat stand. *Agric. For. Meteorol.*, **151**, 345–355, <https://doi.org/10.1016/j.agrformet.2010.11.010>.
- Kay, B. D., and A. J. VandenBygaart, 2002: Conservation tillage and depth stratification of porosity and soil organic matter. *Soil Tillage Res.*, **66**, 107–118, [https://doi.org/10.1016/S0167-1987\(02\)00019-3](https://doi.org/10.1016/S0167-1987(02)00019-3).
- Kozak, J. A., L. R. Ahuja, T. R. Green, and L. Ma, 2007: Modelling crop canopy and residue rainfall interception effects on soil hydrological components for semi-arid agriculture. *Hydrol. Processes*, **21**, 229–241, <https://doi.org/10.1002/hyp.6235>.
- Kucharik, C. J., and K. R. Brye, 2003: Integrated Biosphere Simulator (IBIS) yield and nitrate loss predictions for Wisconsin maize receiving varied amounts of nitrogen fertilizer. *J. Environ. Qual.*, **32**, 247–268, <https://doi.org/10.2134/jeq2003.2470>.

- , and T. E. Twine, 2007: Residue, respiration, and residuals: Evaluation of a dynamic agroecosystem model using eddy flux measurements and biometric data. *Agric. For. Meteorol.*, **146**, 134–158, <https://doi.org/10.1016/j.agrformet.2007.05.011>.
- , and Coauthors, 2000: Testing the performance of a dynamic global ecosystem model: Water balance, carbon balance, and vegetation structure. *Global Biogeochem. Cycles*, **14**, 795–825, <https://doi.org/10.1029/1999GB001138>.
- , A. VanLoocke, J. D. Lenters, and M. M. Motew, 2013: Miscanthus establishment and overwintering in the Midwest USA: A regional modeling study of crop residue management on critical minimum soil temperatures. *PLoS One*, **8**, e68847, <https://doi.org/10.1371/journal.pone.0068847>.
- Lamari, L., 2008: Assess 2.0: Image analysis software for plant disease quantification. American Phytopathological Society.
- Li, X., J. Niu, and B. Xie, 2013: Study on hydrological functions of litter layers in north China. *PLoS One*, **8**, e70328, <https://doi.org/10.1371/journal.pone.0070328>.
- Liang, X., and J. Guo, 2003: Intercomparison of land-surface parameterization schemes: Sensitivity of surface energy and water fluxes to model parameters. *J. Hydrol.*, **279**, 182–209, [https://doi.org/10.1016/S0022-1694\(03\)00168-9](https://doi.org/10.1016/S0022-1694(03)00168-9).
- Lokupitiya, E., and Coauthors, 2009: Incorporation of crop phenology in Simple Biosphere Model (SiBcrop) to improve land-atmosphere carbon exchanges from croplands. *Biogeosciences*, **6**, 969–986, <https://doi.org/10.5194/bg-6-969-2009>.
- Lundberg, A., M. Eriksson, S. Halldin, E. Kellner, and J. Seibert, 1997: New approach to the measurement of interception evaporation. *J. Atmos. Oceanic Technol.*, **14**, 1023–1035, [https://doi.org/10.1175/1520-0426\(1997\)014<1023:NATTMO>2.0.CO;2](https://doi.org/10.1175/1520-0426(1997)014<1023:NATTMO>2.0.CO;2).
- Mahfouf, J. F., and J. Noilhan, 1991: Comparative study of various formulations of evaporations from bare soil using in situ data. *J. Appl. Meteorol.*, **30**, 1354–1365, [https://doi.org/10.1175/1520-0450\(1991\)030<1354:CSOVFO>2.0.CO;2](https://doi.org/10.1175/1520-0450(1991)030<1354:CSOVFO>2.0.CO;2).
- Mo, K. C., L. N. Long, Y. Xia, S. K. Yang, J. E. Schemm, and M. Ek, 2011: Drought indices based on the climate forecast system reanalysis and ensemble NLDAS. *J. Hydrometeorol.*, **12**, 181–205, <https://doi.org/10.1175/2010JHM1310.1>.
- Moreira, V. S., and Coauthors, 2015: Seasonality of soil water exchange in the soybean growing season in southern Brazil. *Sci. Agric.*, **72**, 103–113, <https://doi.org/10.1590/0103-9016-2014-0056>.
- Olivier, F., and A. Singels, 2012: The effect of crop residue layers on evapotranspiration, growth and yield of irrigated sugarcane. *Water SA*, **38**, 77–86, <https://doi.org/10.4314/wsa.v38i1.10>.
- Peel, M. C., B. L. Finlayson, and T. A. McMahon, 2007: Updated world map of the Köppen-Geiger climate classification. *Hydrol. Earth Syst. Sci.*, **11**, 1633–1644, <https://doi.org/10.5194/hess-11-1633-2007>.
- Pollard, D., 1995: Use of a land-surface-transfer scheme (LSX) in a global climate model: The response to doubling stomatal resistance. *Global Planet. Change*, **10**, 129–161, [https://doi.org/10.1016/0921-8181\(94\)00023-7](https://doi.org/10.1016/0921-8181(94)00023-7).
- Reichert, J. M., L. E. A. S. Suzuki, D. J. Reinert, R. Horn, and I. Håkansson, 2009: Reference bulk density and critical degree-of-compactness for no-till crop production in subtropical highly weathered soils. *Soil Tillage Res.*, **102**, 242–254, <https://doi.org/10.1016/j.still.2008.07.002>.
- Reichstein, M., and Coauthors, 2005: On the separation of net ecosystem exchange into assimilation and ecosystem respiration: Review and improved algorithm. *Global Change Biol.*, **11**, 1424–1439, <https://doi.org/10.1111/j.1365-2486.2005.001002.x>.
- Schwartz, R. C., R. L. Baumhardt, and S. R. Evett, 2010: Tillage effects on soil water redistribution and bare soil evaporation throughout a season. *Soil Tillage Res.*, **110**, 221–229, <https://doi.org/10.1016/j.still.2010.07.015>.

- Song, Y., A. K. Jain, and G. F. McIsaac, 2013: Implementation of dynamic crop growth processes into a land surface model: Evaluation of energy, water and carbon fluxes under corn and soybean rotation. *Biogeosciences*, **10**, 8039–8066, <https://doi.org/10.5194/bg-10-8039-2013>.
- Tormena, C. A., M. C. Barbosa, A. C. S. da Costa, and C. A. Gonçalves, 2002: Densidade, porosidade e resistência à penetração em latossolo cultivado sob diferentes sistemas de preparo do solo. *Sci. Agric.*, **59**, 795–801, <https://doi.org/10.1590/S0103-90162002000400026>.
- Twine, T. E., J. J. Bryant, K. T. Richter, C. J. Bernacchi, K. D. McConnaughay, S. J. Morris, and A. D. B. Leakey, 2013: Impacts of elevated CO<sub>2</sub> concentration on the productivity and surface energy budget of the soybean and maize agroecosystem in the Midwest USA. *Global Change Biol.*, **19**, 2838–2852, <https://doi.org/10.1111/gcb.12270>.
- van Donk, S. J., D. L. Martin, S. Irmak, S. R. Melvin, J. L. Petersen, and D. R. Davison, 2010: Crop residue cover effects on evaporation soil water content, and yield of deficit-irrigated corn in west-central Nebraska. *Trans. ASABE*, **53**, 1787–1797, <https://doi.org/10.13031/2013.35805>.
- Vanloocke, A., C. J. Bernacchi, and T. E. Twine, 2010: The impacts of *Miscanthus* × *giganteus* production on the Midwest US hydrologic cycle. *GCB Bioenergy*, **2**, 180–191, <https://doi.org/10.1111/j.1757-1707.2010.01053.x>.
- Van Wijk, W. R., and D. A. DeVries, 1963: Periodic temperature variations in a homogeneous soil. *Physics of the Plant Environment*, W. R. Van Wijk, Ed., Wiley, 102–143.
- Verkler, T. L., K. R. Brye, E. E. Gbur, J. H. Popp, and N. Amuri, 2008: Residue management and water delivery effects on season-long surface soil water dynamics in soybean. *Soil Sci.*, **173**, 444–455, <https://doi.org/10.1097/SS.0b013e31817b6687>.
- Webb, E. K., G. I. Pearman, and R. Leuning, 1980: Correction of flux measurements for density effects due to heat and water vapour transfer. *Quart. J. Roy. Meteor. Soc.*, **106**, 85–100, <https://doi.org/10.1002/qj.49710644707>.
- Webler, G., D. R. Roberti, S. V. Cuadra, V. S. Moreira, and M. H. Costa, 2012: Evaluation of a dynamic agroecosystem model (Agro-IBIS) for soybean in southern Brazil. *Earth Interact.*, **16**, 1–15, <https://doi.org/10.1175/2012EI000452.1>.
- Wei, Z., P. Paredes, Y. Liu, W. W. Chi, and L. S. Pereira, 2015: Modelling transpiration, soil evaporation and yield prediction of soybean in North China Plain. *Agric. Water Manage.*, **147**, 43–53, <https://doi.org/10.1016/j.agwat.2014.05.004>.
- Wyngaard, J. C., 1990: Scalar fluxes in the planetary boundary layer—Theory, modeling, and measurement. *Bound.-Layer Meteor.*, **50**, 49–75, <https://doi.org/10.1007/BF00120518>.